Proceeding of the IEEE
International Conference on Robotics and Biomimetics
Dali, China, December 2019

Bionic Architecture Design and Robust Rough-Terrain Locomotion for a High-Payload Quadrupedal Robot*

Jing Lin[1,3], Ganyu Deng[1,2], Lu Chen[1,3], Bingchen Jin[1,2], Caiming Sun[1,2,3,a)], Aidong Zhang[1,2,3]
[1]*Institute of Robotics and Intelligent Manufacturing (IRIM), the Chinese University of Hong Kong (CUHK), Shenzhen, China*
[2]*Shenzhen Institute of Artificial Intelligence and Robotics for Society (AIRS), Shenzhen, China*
[3]*Robotics Research Center, Peng Cheng Laboratory, Shenzhen, China*
[a)]Corresponding Author: Dr. Caiming Sun, cmsun@cuhk.edu.cn

***Abstract* - In this work, an electrically actuated quadrupedal robot with bionic architecture, Pegasus, is reported. With investigating the anatomical skeleton of medium-sized dog, its movement mechanism, and dog's joints, we conclude that the architecture design of quadrupedal robots can benefit from bionics research. There is an optimization for structural parameters, geometrical relationship, and motion range of each joint according to the findings in bionics. The bionic structure design is verified by analyzing mechanical performance and motion ability of the robot. The bionic architecture allows COG trajectory not to follow the terrain profile and COG fluctuations are significantly suppressed when going through rough terrains. In order to generate a stable COG trajectory with fewer pose fluctuations, the step sequence and four footholds in each step follow the typical biological gait pattern for dynamic walking over rough terrains while the robot can keep robust postures in efficient workspace for each leg. Moreover, "Virtual Muscle" model is realized for each leg's compliance control with two sets of virtual spring and damper, in order to absorb feet impacts on the ground.**

Index Terms - quadrupedal robot, bionic robot, locomotion, center of gravity (COG).

I. INTRODUCTION

Legged robots are superior to tracked and wheeled robots for applications of traversing rough terrains and obstacle-crossing in complicated environments due to their higher freedom of foothold selection. The quadruped robot performs better than biped and hexapod robot [1, 2], in terms of speed, loading ability, stability, robustness, and obstacle crossing. Quadruped robots are mainly designed to imitate the structure of mammals in nature since quadruped animals (cheetah, dog, horse, etc.) have excellent performance in moving speed and environmental adaptability. Also, there are various gait patterns and free footholds, which can be used to overcome the impact of complex terrains on robot stability, and also to achieve high-speed movement in dynamic conditions. They are very suitable to aid humans in the performance of tasks in complex unstructured environments such as rescue, reconnaissance and extra-terrestrial exploration [3-5].

Up to now, many quadruped robots have been developed to imitate quadruped mammals. The most famous hydraulic quadruped robot is Boston Dynamics' BigDog [1, 6], weighing 109 kg. Powered by conventional fuel with high energy density, it has high mobility and environmental adaptability, but the robot made by bulky hydraulic drive system components cannot be miniaturized (normally 50~100 kg, or even higher), needs complex control system, and generates smoke and noise, nearly impossible to work together with humans friendly. Another group of quadrupedal robots actuated by electric motors, such as SpotMini developed by Boston Dynamics, ANYmal [7], StarlETH [8], and Cheetah 3 [9], are lighter, only weighing 20~30 kg, and more flexible in structure. Therefore, electrically actuated quadruped robots are much closer to their biological counterpart, the medium-sized dog (25 kg) [10], with significant advantages of light weight, flexible structure, good dynamic performance, quietness, no smoke emissions, etc, attracting more and more research interest in recent years.

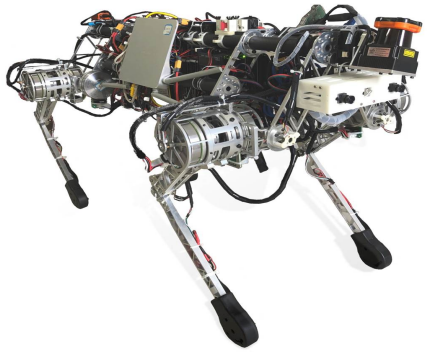

Fig. 1 Pegasus, a quadruped robot with bionic architecture.

Although researchers are working hard to improve energy efficiency when quadruped robots transport high payload over rough terrains, the performance of quadruped robots cannot perform so efficiently as the natural biological counterparts yet [10] and the power to weight ratio of most medium-sized quadruped robot is low. One of the reasons for this low efficiency is because there isn't enough attention paid to the overall architecture of mammal skeleton [11] when imitating animals since the bionic architectures are very critical for quadruped robots to get an optimized weight and volume while

* This work is in part supported by the National Natural Science Foundation of China (Grant No. U1613223), in part by the Shenzhen Natural Science Foundation (Grant No. JCYJ20180508163015880), and in part by funding from Shenzhen Institute of Artificial Intelligence and Robotics for Society.

978-1-7281-6321-5/19//$31.00 ©2019 IEEE

they are stressing, get reasonable workspace, improve stability, and choose pose for excellent adaptive behaviours as their biological counterparts [12]. On the other hand, to date no energy-efficient locomotion strategy is proposed for robust and smooth movements over challenging terrains with fewer center of gravity (COG) fluctuations and pose alternations. How would we plan a locomotion trajectory for the quadruped robots to efficiently go across such rough terrains? Conventionally, the desired COG positions of quadruped robots follow the terrain profile, such as LittleDog [13] and ANYmal [7], meanwhile, plenty of energy is consumed to tolerate COG fluctuations and pose alternations. Recently, a significant progress has been made in the control of COG, particularly in the realization of dynamic locomotion in several wheeled-legged robots. These robots can go across challenging terrain with fewer COG fluctuations, such as wheeled ANYmal [14] and the Handle robot from Boston Dynamics Company.

In this work, we present Pegasus, an electrically actuated quadrupedal robot imitating the medium-sized dog, as shown in Fig. 1. Bionic architecture is designed based on a careful investigation of anatomical skeleton for medium-sized dogs, which makes its mechanical strength and workspace fully optimized. Furthermore, a low-torque area throughout the whole workspace for hip and knee joints is found out for robust locomotion. Finally, "Virtual Muscle" model for each leg and biological gait patterns are utilized to realize the stable COG trajectory with fewer pose fluctuations, when walking across rough terrain.

II. BIONIC QUADRUPED ROBOT SYSTEM DESIGN

A. Overview of quadruped robot Pegasus

With natural selection and evolution for millions of years, animals have excellent environmental adaptability. And the skeletal structure, components and muscles density distribution of modern mammals have been perfectly organized with strong rationality on energy conversion, locomotion strategy, and the selection of gaits and gestures [15-18]. The structural design for quadruped robot can find critical reference from the skeleton structure of animals, especially quadruped mammals like dog, horse, cheetah, etc.

The overall structure of our quadruped robot Pegasus is constructed modularly from the main body, four legs with almost the same structure and the same layout, the motor drivers, related sensors and the embedded system. While standing in the initial posture , its length and width are about 0.9 m and 0.56 m respectively, similar to a medium-sized dog. The thigh length is 0.26 m, and the shank length is also 0.26 m with additional 8 cm diameter foot. The total weight of the robot is 30 kg.

Rotating Hokuyo UTM-30LX sensors provide a three-dimensional perception of the environment. Each leg has three individual degrees of freedom (DOF), corresponding to 3 joints on each leg. Each joint is actuated by one high-power electric motor integrated with a harmonic gear. Angle encoders are equipped into each joint, and the current and velocity of the motor are measured as the force feedback and power consumption of each joint. In order to ensure the structural strength and minimize the weight of the robot, carbon fibre tubes are applied to the main body as a skeleton and the remaining majority of mechanical parts are made of a strong Aluminum alloy (type 7075). Then, the final architecture of our robot is quite similar to the anatomical structures of dog skeleton.

B. Bionic architecture

Our robot is expected to meet the requirements for carrying payloads in assistance of humans and good adaptability for unstructured terrains. With carefully comparing typical quadruped animals, we find that the dogs are good at speed and endurance, suitable for bearing load and hiking. Therefore, we choose an adult medium-sized dog as a biomimetic reference and design the robot structure by summarizing structural features and movement rules of bones.

The dog contains 225~230 bones, which play a role in supporting the body, maintaining body shape, protecting internal organs and attaching muscles. The primary function of legs is to move and sustain the body. Front legs sustain most of the body weight; in contrast, the hind legs contribute most of the forward propulsion. The front leg is mainly composed of five parts: scapula, humerus, radius, metacarpus, and phalanges. The hind leg is also mainly composed of five parts: sacrum, femur, tibia, metatarsus, and phalanges. There are tough tendons at the end of radius which not only entangle the metacarpal and phalangeal bones but also allow them to move flexibly. Meanwhile, this structure can effectively absorb vibration and increase elasticity, improving the efficiency of movement while running. The metacarpus/metatarsus and phalanges are equivalent to the foot of the robot, and we design a rubber mat structure with flexible force senor embedded to simulate it. These bones and main body are connected together by turning joints. Dog's movement is controlled by nerves, and coordinated by muscles, bones and joints. Muscles are the motive force, bones are the lever of movement, and joints are the pivot.

We categorized and named the bone of dog leg in Fig. 2a. Our robot Pegasus is designed based on a careful investigation of anatomical skeleton for medium-sized dogs. Since it is difficult for the robot to completely imitate such complex structures of a real dog, we will simplify the anatomical skeleton reasonably, translate these skeletal structure to the actual size of the robot system, and eventually obtain the dimensions of all parts, such as thigh (*L1*), shank (*L2*), vertebrae (*L3*), scapula (*L4*), and shoulder (*L5*) as close as possible to the anatomical structure of dog skeleton in Fig. 2b. The dimensions of dog and Pegasus are shown respectively in Table I. It is found that the robot architecture has all critical segments of thigh, shank, vertebrae, scapula, and shoulder corresponding to the equivalent structures of dog skeleton.

C. Leg structure

Normally, at least three active degrees of freedom are

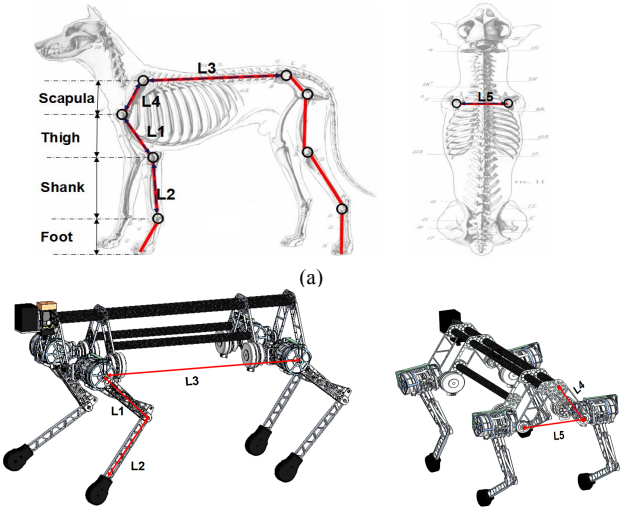

Fig. 2 (a) Divisions of bone structure of medium-sized dog, (b) Segmentation of Pegasus robot structure.

TABLE I
Dimension of bone segments

Architecture	Thigh L1	Shank L2	Vertebrae L3	Scapula L4	Shoulder L5
Dog study (a.u.)	41	45	103	25	30
Pegasus robot (mm)	260	260	740	186	237

required to place the foot in a three-dimensional space. Here each leg is actuated by three joints. As for the leg module design, we adopt the design principle of low inertia leg and place both the knee actuator and hip actuator at the hip joint as shown in Fig. 3. Besides, a four-bar-linkage mechanism is used to deliver the knee actuator's torque to knee joint. Thus, the overall COG is located close to the hip joint which will reduce the inertial momentum of the whole leg. The two joints in the leg-sagittal plane are called hip flexion / extension (HFE joint) and knee flexion / extension (KFE joint). The third joint is called hip abduction / adduction (HAA joint). Each joint comprises a brushless motor and a harmonic gearbox, meanwhile, the position encoders which servo the motor are mounted inside the motor and outside the joint. For instance, each motor has an incremental encoder mounted in the motor and an absolute customized magnetic encoder mounted outside the joint. The mechanical parts of the leg are made of lightweight aeronautic aluminum materials (Aluminum alloy 7075), which can not only provide enough strength for the leg, but also reduce the structure weight. The cover of the foot is made of rubber which is fixed at the end of foot can absorb impacts between foot and ground. The total weight of one leg module is almost 3.8 kg, including the HAA joint, HFE joint, and the KFE joint.

Similar to the anatomical skeleton, the HAA joint connects the vertebra and scapula / sacrum and acts on side swing the whole leg. The HFE joint connects the scapula/sacrum and thigh and acts on the thigh lifting. The

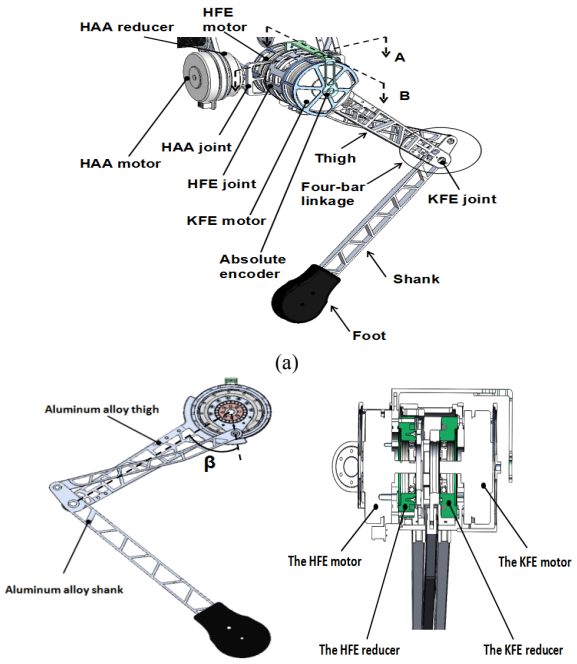

Fig. 3 (a) Leg structure of Pegasus robot, (b) A cutaway view of the leg, the four-bar linkage structure of the leg (c) B cutaway view of the leg.

KFE joint connects the thigh and shank and acts on shank lifting.

D. *Software configuration*

The remote and central PCs share the tasks of the locomotion, navigation and remote control on the robot. Navigation data is transferred over the network by the Robot Operating System (ROS) running on a low-latency patched Ubuntu 16.04. The ROS master, which manages the connections between the different processes. The locomotion process, the real-time critical whole-body controller and state estimator are timed by the CAN driver that communicates with the actuator units at 200 Hz. The readings and commands are exchanged through shared memory and publish time-critical workers like the foothold planner. The localization and mapping tasks are conducted on the navigation module using LIDAR-based and camera-based sensors for the unstructured environments. High-level navigation tasks are coordinated by a mission planner and executed by a path planner that sends velocity commands to the locomotion controller via pipes between locomotion and navigation processes.

III. Influence of Bionic Architecture on Robot Performance

A. *Mechanical system performance analysis*

As well known, the mass and architecture of dog skeleton are optimized to the excellent stabilization when facing externally mechanical stimuli [19]. We introduced the idea of bionic architecture in the stage of robot structure design, study the proportion of fuselage reasonably, and plan the gait space properly for the purpose of reducing weight and improve efficiency while maintaining the overall strength, stiffness, and

stability of the whole structure. In order to fully verify the reliability of the bionic structure, the dynamic and static analysis of the whole robot and the single leg including all key components are carried out.

1) Torque requirements for hip flexion / extension joint (HFE joint) and knee flexion / extension joint (KFE joint): Cooperative movement between the HFE joint and KFE joint constructs leg postures while robot is walking or stepping over obstacles. We analyze the variation trend of output torque for HFE joint and KFE joint in the motion range of all leg joints, while robot standing up and being fallen down.

In the rotation process of HFE joint, when the HFE joint turns to a different angle position (*des0*), the robot's thigh will go to the corresponding position. When the KFE joint turns to a different angle position (*des1*), the robot's shank will also go to the different position accordingly, and the β (shown in Fig. 3b) corresponds to the different value. In the process of KFE joint rotation, the transformation relationship between β and *des1* is as follows:

$$des1 = \alpha - \beta . \qquad (1)$$

Where α a control constant, set as 1.5789.

Therefore, a set of data consisting of the HFE joint position (*des0*) and the KFE joint position corresponds to a specific leg posture. The postures of the four legs are the same. Thus the body height of the robot can be adjusted by controlling the leg in different leg posture.

Set the leg in different posture in a simulation environment and the mechanical performance is analyzed accordingly. And the main body (including the built-in hardware systems plus some payloads) weight of the robot is set to 20 kg, and the mass of each leg is set to 3.8 kg.

In one analysis process, fixing the value of *des0*, change the value des1 to control the shank from the limited position of stretch to that of the flexion. The value of *des0* increases by 5° for each analysis process, in the range from 0 to 90°. Fig. 4 depicts the variation trend of output torque for HFE joint and KFE joint throughout the whole workspace.

Those results show that the larger *des0*, the greater the angle between the thigh and the vertical line; the smaller *des1*, the greater the degree of leg stretch is; the smaller the output torque of joint is, and more efficiently the robot walks. Both KFE joint and HFE joint are analyzed in the process of robot standing up. Moreover, our simulation model of the entire robot system taking into account the interaction between the various components of the whole system, which is closer to the actual situation of the robot. In an analysis of the change of the shank from the flexion limit position to the extension limit position when the thigh is fixed, the variation trend of the joint torque for the knee joint is obtained, which reaches the maximum value at the flexion limit position. Since we analyze HFE joints at the same time, we can simultaneously observe the torque changes of the two joints at different postures of the thigh.

2) Structural strength analysis: In order to simulate the static structure strength of each part of a single leg as realistic

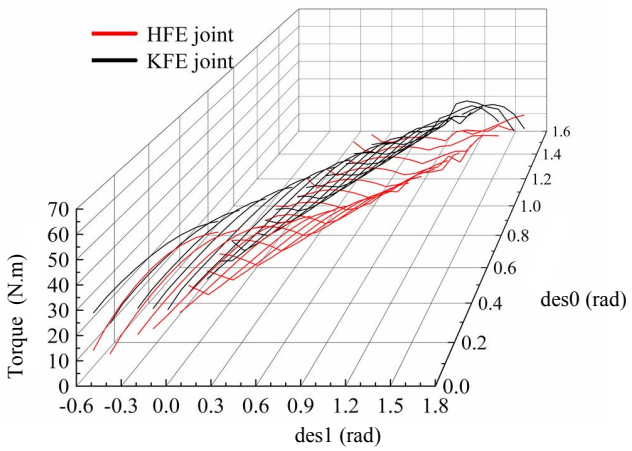

Fig. 4 Output torque for HFE joint and KFE joint throughout the whole workspace.

as possible, and to fully verify the reliability of robot leg structure, we analyze the single leg system especially. As shown in Fig. 4, the requirement of structural strength is highest when the leg posture is (0, 0.35), where the angle between the thigh and the vertical line is minimized (*des0=0*), and the shank is at the limited position of flexion (*des1*=0.35). We use the ANSYS software to analyze the static structure strength of the leg when the leg is in the posture of (0, 0.35). The load of the single leg is set as 90 N, heavier than the quarter gravity of the robot system. The force is applied to the bearing hole which connects the leg and the main body frame (the axis of the HAA joint). And the force vector is both perpendicular to the ground and the axis of HAA joint. Fixing the contact surface of robot foot and ground, other constraints and materials of this model in a simulation are the same as the prototype of robot.

Fig. 5 shows the result of the finite element model (FEM) analysis for the hardest case of leg posture of (0, 0.35). The maximum deformation of 1.1482 mm appears near the bearing hole of the hip-swinging plate (Fig. 5b). Compared to the overall dimension of the leg, the deformation can be considered within the acceptable range.

The maximum stress of 413 Mpa appears on the corner grooves of disk which connects the HFE joint reducer and leg sleeve (Fig. 5c), less than the yield strength of Aluminum alloy 7075. The stress value of other parts is very small (no more than 45 Mpa), which indicates the overall reliability of the single leg system is high.

As the carrier of leg movement, the robot's main body structure bears complex force and large torque. The control system, actuators, batteries, sensors, and loadings are all installed within main body. To ensure that the design meets requirements for structural strength and stiffness and verify the reliability of mechanical design under interactions of all parts, we also made an analysis of the robot's overall mechanical system. Use ANSYS software to analyze the static structure strength of the whole robot when four legs are at the most dangerous posture of (0, 0.35). As depicted in Fig. 6a the load is set as 200 N similar to the main body gravity of the

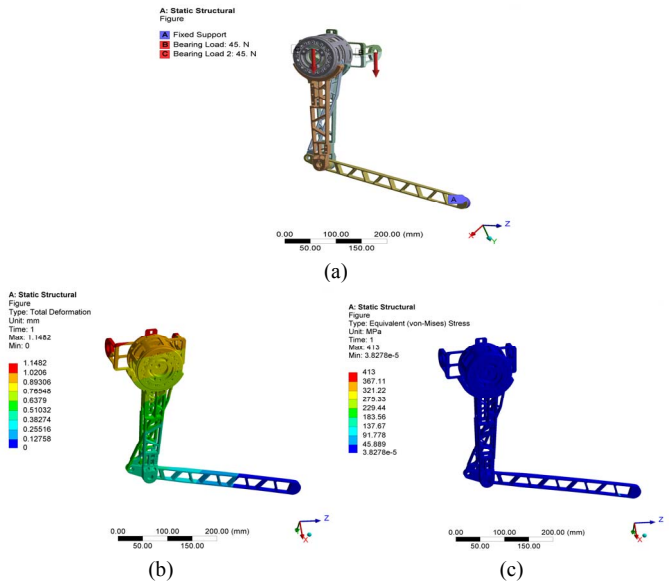

(a)

(b) (c)

Fig. 5 Structural deformation and stress analysis of the single leg. (a) the finite element model of the leg, (b) the total deformation of the leg (c) the equivalent stress of the leg.

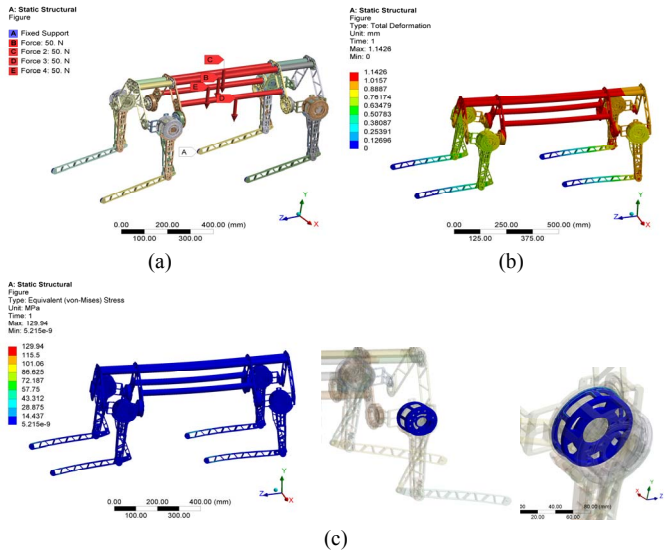

(a) (b)

(c)

Fig. 6 Structural deformation and stress analysis of the whole robot. (a) the finite element model of the robot, (b) the total deformation of the robot (c) the equivalent stress of the robot.

robot system (including the built-in hardware systems plus some loadings). The force is uniformly applied to the middle position of the four bearing rods of the robot body frame. And the force vector is both perpendicular to the ground and the bearing rod. Fixing the contact surfaces of robot foot and ground, other constraints and materials of this model in a simulation are the same as the robot prototype.

As shown in Fig. 6b, the maximum deformation of 1.1426 mm appears on the four bearing rods, connection parts which connect the main body and four legs, and the knee joint of the rear legs of the robot. The overall deformation is very small which indicates that the stiffness of the robot is very good. The maximum stress appears on the edges of leg sleeves and disks which connect the HFE joint reducer and leg sleeve, the value is 129.94 Mpa (Fig. 6c). The maximum stress locates where it appears in the single leg analysis (Fig. 6c), but it is less than that in the single leg analysis, which indicates that interconnection parts of the whole robot improves the reliability of the system. Furthermore, the value 129.94 Mpa is less than the yield strength of Aluminum alloy 7075 (503 Mpa). The stress value of other parts is less than the yield strength of their material. The minimum safety factor is 4.1, greater than the normal value of 3. It shows that the mechanical design of the overall structure of the robot can fully meet the static stiffness and strength requirements under the most extreme working conditions although the proportions of our parts are slightly different from those of the actual dog. Also, every position of mechanical parts of the robot can be replaced by the material of higher strength to adapt the greater loadings.

B. Motion ablity analysis

As mentioned above, our robot architecture is based on bio-skeleton with mechanical limitations of hardware system. The proportion of robot structure and the ranges of leg joints are different from those of the real dog. In order to verify the bionic structure of the robot is feasible in real applications, we not only need to check whether the robot system is strong enough under extremely mechanical stress but also to know whether its motion ability is satisfied to efficiently go across rough terrains. Since workspace is directly relevant to the ability of leg moving, here we use the area of workspace as a method to characterize the robot motion ability.

1) Joint motion range and workspace: Charles D. Newton had researched the joint ranges of ten mixed breed dogs [20]. According to his research, the abduction-adduction of the shoulder is depicted in Fig. 7a, and A means zero starting position: the dog is in lateral recumbency or standing, and the shoulder is in 45° extension.

Two U-shape-plate structures are designed to imitate the scapula to reduce the complexity of our robot. So we set the zero position as the axis of HFE joint perpendicular to the forward direction of the robot when the leg touches downwards. B abduction: the outward motion (abaxial) from the zero starting point. C adduction: the inward motion (axial) from the zero starting. The hip flexion-extension is depicted in Fig. 7b, and A means zero starting position: with the animal in lateral recunbency, the femur is positioned to be at right angles to a line connecting the tuber sacrale and tuber ischi of the pelvis. As mentioned above, since the structure of the scapula of our robot has been simplified, we set the zero position as the thigh in the vertical position. B means the limited flexion position and C means the limited extension position. The knee flexion and extension are depicted in Fig. 7c, and A means zero starting position: the tibial axis is held at a right angle to the femoral axis. Similarly, we set the position of the thigh in the vertical position and the thigh perpendicular to the shank as the zero position to our robot. B means the limited flexion position and C means the limited extension position. Hyperextension is measured in degrees occurring after the knee has extended 90°. The zero position of the robot

TABLE II
Motion range of all joints

Joint	Dog research	Pegasus robot
The shoulder abduction/adduction	40°-50° / 40°-50°	170°/180°
The hip flexion/extension	70°-80° / 80°-90°	150°/150°
The knee flexion/extension	65°-75° / 65°-75°	47.91° / 90°

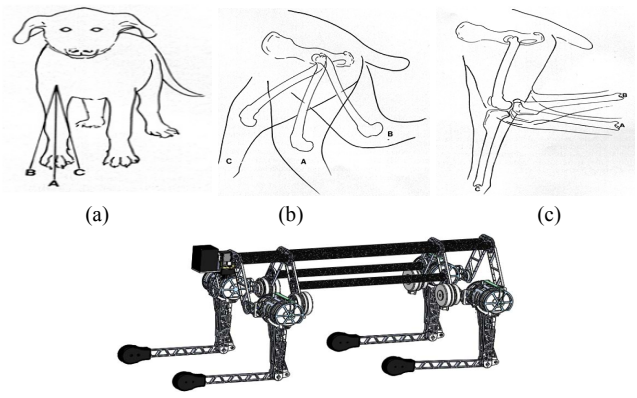

(a) (b) (c)

(d)

Fig. 7 The motion ranges of leg joints.

in three cases is shown in Fig. 7d.

The motion range of each joint determines the gaits and workspace of the robot. Too small range of joints will lead to the decline of robot motion ability and efficiency; too large range of joint motion will induce mechanical interference, motion singularity, or other issues, so the range of motion is very important for functional quadruped robots. Combined the real canine model with the hardware system, our robot are designed to maximize the joint ranges. For example, to get a wider abduction range movement of the joint, the axle of HAA is deviated outwards, which helps the thigh to get a quite large range of motion. Finally, the motion ranges of Pegasus robot and breed dogs are shown respectively in Table. II.

Workspace refers to the area that the end of the leg can reach, called "reachable workspace", which is determined by the motion ranges of leg joints and the length of each leg segment.

We obtained the workspace by analyzing the forward kinematics of single leg structure, based on ground reaction force (GRF) of about 100 N extracted from our robot walking experiments. Set the motion range of the leg joints as shown in Table II: the hip flexion/extension (the HFE joint): 150°/150°, the knee flexion/extension (the KFE joint): 47.91°/90°and the HAA joint is in the zero starting position. The workspace of the robot leg calculated by Matlab is shown in Fig. 8a.

From the calculated workspace diagram (Fig. 8a), we can see that except for the middle circle inaccessible region caused by the dead-point region of the four-bar-linkage, the whole motion space is still relatively large, which basically covers all kinds of gait and posture during the normal walking and obstacle-crossing process of the robot, and the motion ability of the robot is relatively high.

2) Joints torque distribution for robust walking over rough terrains: In order to figure out robust postures of the leg, we further analyze the torque distribution throughout the reachable workspace for Pegasus robot. Fig. 8b and Fig. 8c depict the torque distribution for HFE joint and KFE joint when the load of one leg equals to 100 N in the vertical direction, where Torque1 and Torque2 represent the torque of leg joints, HFE and KFE respectively. Fig. 8b shows that the distribution of HFE torque behaves as a mirror symmetry along a vertical line (X=0), the bluest region in the graph, and the farther the foot end goes away from this line, the higher torque the joint need provide. The white dot lines at X= -0.3 m and X= +0.3 m correspond the nominal value of HFE joint torque (about 27 N.m) for this leg, meaning that when the leg moves in the range of X (-0.3 m, +0.3 m), Torque1 lies in a continuous operation region below the nominal value. The nominal value for joint torque is relying on the continuous region for motor currents, exhibiting the loading capability of the joint actuator. It needs to mention that the workspace of HAA is very similar to that of HFE. Therefore, HAA joint will not be discussed here in details.

Meanwhile, the torque distribution of KFE joint is shown in Fig. 8c and it is found that all values of KFE torque are below the nominal joint torque (27 N.m) for our bionic design of leg structure. This bionic behavior is pretty meaningful for legged robots since the knee joints will encounter the major part of foot impact when legs strike the ground. The minimum KFE torque is tracing the two bluest curves in the first quadrant and third quadrant of reachable workspace. Considering the combination of HFE torque and KFE torque on a leg, an energy-efficient workspace is found out to situate in region between the bluest curve in Fig. 8c and the line at X=0 marked by black dot lines in the third quadrant, called as "efficient workspace".

Fig. 9 shows that the reachable workspace is maximized as the length of thigh ($L1$) equals to that of shank ($L2$), corresponding to the bionic design in Fig. 2 and Table I. When the ratio deviates from 1:1 further and further, the ring area of reachable workspace becomes narrower and narrower. We also investigate the influence of leg segments ratio on the torque distribution for HFE joint and KFE joint. In Fig. 9a, the symmetric behavior for HFE torque for different leg segments ratios is similar to that shown in Fig. 8b. The mirror symmetry is maintained and two white dot lines for the nominal joint torque (27 N.m) always situate at X= -0.3 m and X= +0.3 m. In contrast, the torque distribution becomes worse and worse as thigh to shank deviates from 1:1 ratio shown in Fig. 9b, where the KFE joint torque exceeds the the nominal value as marked by white dot lines. So the bionic architecture for our robot is greatly benefitting from efficient locomotion of dog according to the findings of [21].

C. Robust locomotion for bionic quadruped robots over rough terrains

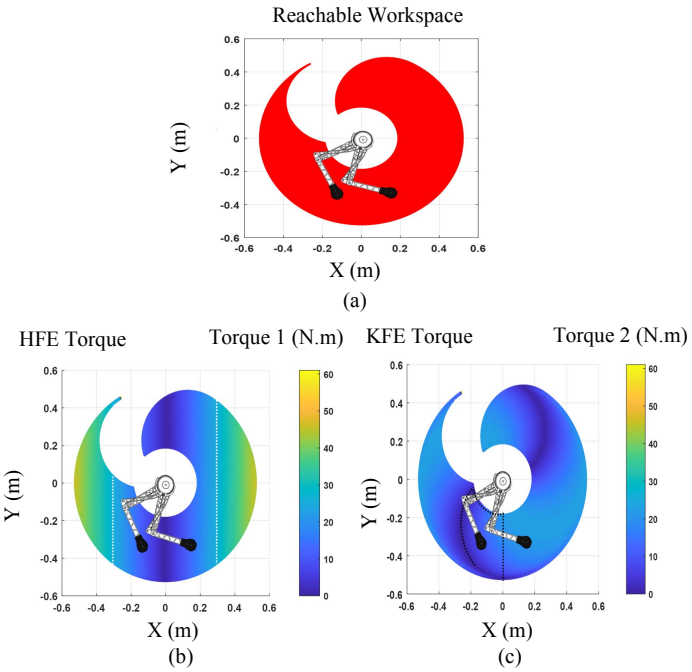

Fig. 8 (a) The reachable workspace for Pegasus leg, (b) the HFE joint torque in different postures, (c) the KFE joint torque in different postures throughout the whole reachable workspace.

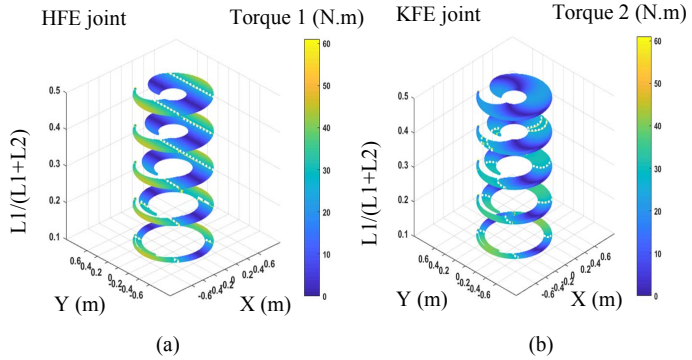

Fig. 9 Dependence of workspace and torque distribution on leg segments ratio of thigh (L1) and shank (L2) for the HFE joint (a) and the KFE joint (b).

From above analysis of mechanical performance and motion ability, the bionic architecture can provide enough reachable workspace for legs and also create an efficient workspace combining the torque distribution for HFE and KFE joints. Using this efficient workspace for each leg, we can plan a robust rough-terrain locomotion for quadrupedal robots. It is critical for legged robot to find suitable footholds when it efficiently traverses rough terrains [22, 23]. Imitating the walking steps for quadruped mammals (dog, cat, horse, etc.), a series of steps with different stride length is simultaneously planned based on the given terrain and kinematic constraints. Given a desired path for the robot's COG, the step sequence of the planning process is to plan a set of footsteps that follow this path. The COG trajectory generator uses the next sequence of four footholds, which follow the standard biological gait pattern for dynamic walking. The swing leg sequence is called "double support triangle" sequence [22, 24, 25], and each leg is controlled by dynamic compliance with two sets of virtual spring and damper [26], called "Virtual Muscle" model. Eventually, we planned a stable COG trajectory with fewer pose fluctuations and realize an robust locomotion for bionic quadruped robots.

1) Bionic walking with artificial elasticity of each leg: In nature, typical quadruped gaits have been found, such as walking, trotting, bounding, or galloping. There have been plenty of bio-inspired hints that animals instinctively choose the gait and preferred forward speed to minimize energy consumption and to avoid injuries generated by excessive musculoskeletal forces when animals walk over rough terrains or go across challenging obstacles [27, 28]. The walk has been identified as the least tiring and most efficient form of locomotion of the dog when crossing over complex terrains such as forest, desert and debris. During walking, the dog never has fewer than two feet on the ground (usually three feet), and occasionally all four feet may be on the ground [29]. In this work, quadruped robot uses the bionic walking gait for robust locomotion over rough terrains.

A compliance control method is introduced to each leg to provide artificial elasticity [26, 30]. It contains two sets of virtual spring and damper: one is defined along horizontal direction, and the other is defined in vertical direction, called "Virtual Muscle" model similar to Ref. [31]. This virtual elasticity is very critical for quadruped robots to execute the dynamic walking over challenging terrains, since the leg compliance absorbs most of impulses when food ends hit the uneven ground.

2) Experiments of robustly and smoothly walking over uneven terrains: To develop the science of quadruped robotics toward flexible locomotion over rough terrain, our goal is to plan a COG trajectory for quadruped robot over rough terrain. The locomotion method is tested on unstructured surface such as gaps, steps of varying step heights, and slopes in simulation environment. As similar to Ref. [25], we apply the model in more rough environments. The basic idea of our approach is depicted in Fig. 10a. We wish the COG fluctuations along z-axis (gravitational direction) can be minimized, and the COG trajectory doesn't follow the terrain profile.

It is verified that our planning method is able to traverse a wide variety of challenging terrains at speeds ranging from 0.01 m/s to 0.1 m/s with stable COG trajectory generated by bionic gait patterns. It demonstrates that this locomotion method performs well on rough terrains.

In order to experimentally validate the model and the stability of the algorithm on our robot prototype, we present a dynamic walking gait for robot with total load of 60 kg, robot weight of 30 kg plus payload of 30 kg, to walk on plane ground and uneven ground with obstacles respectively at a speed of 0.042 m/s based on the trajectory planning of COG, as shown in Fig. 10b (more details are shown in supplementary video).

IV. Conclusion

In this work, a robust electrical quadrupedal robot, Pegasus, is presented with a bionic architecture. The energy

efficiency is improved while keeping both mechanical strength of the whole structure and motion ability. In order to

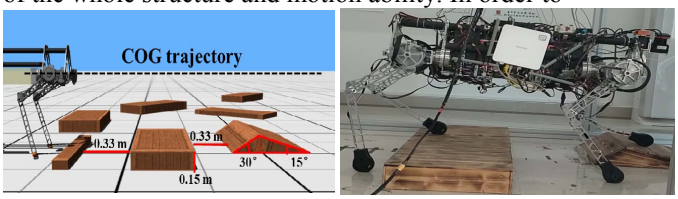

(a) (b)

Fig. 10 (a) Simulation environment for bionic walking with stable COG over rough terrains, (b) Quadruped robot walked over obstacles robustly and smoothly.

get the optimum architecture, the anatomical skeleton for medium-sized dogs is analyzed. The bionic architecture provides good mechanical performance and enough motion ranges of all movable joints, and then motion ability is enhanced when the bionic relationship of leg segments is utilized. That is to say, with the length ratio of thigh to shank of 1:1, the reachable workspace is maximized and the KFE joint torque distribution throughout the whole workspace is kept below the nominal value. Then, bionic walking gaits with virtual compliance control for each leg are utilized for quadruped robot to go across rough terrains. Compared to traditional COG trajectory following the terrain profile, the bionic architecture allows quadruped robot to keep a stable COG trajectory with fewer pose fluctuations, which leads to a robust locomotion through complex obstacles.

REFERENCES

[1] Raibert M, et al. "Bigdog, the rough-terrain quadruped robot." IFAC Proceedings Volumes 41.2 (2008): 10822-10825.

[2] Fukuoka, Yasuhiro, Hiroshi Kimura, and Avis H. Cohen. "Adaptive dynamic walking of a quad-ruped robot on irregular terrain based on biological concepts." The International Journal of Robotics Research 22.3-4 (2003): 187-202.

[3] Saranli, Uluc, Martin Buehler, and Daniel E. Koditschek. "Rhex: A simple and highly mobile hexapod robot." The International Journal of Robotics Research 20.7 (2001): 616-631.

[4] Vernaza, Paul, et al. "Search-based planning for a legged robot over rough terrain." Robotics and Automation, 2009. ICRA'09. IEEE International Conference on. IEEE, 2009.

[5] McGhee, Robert B., and Geoffrey I. Iswandhi. "Adaptive locomotion of a multilegged robot over rough terrain." IEEE transactions on systems, man, and cybernetics 9.4 (1979): 176-182.

[6] Playter R, Buehler M, Raibert M, et al. "BigDog." Proc. of SPIE.2006.

[7] Hutter M, et al. "ANYmal-A Highly Mobile and Dynamic Quadrupedal Robot." International Conference on Intelligent Robots and Systems, pp.38-44, 2016.

[8] Hutter M, Gehring C, Bloesch M, Hoepflinger M, et al. "StarlETH: A compliant quadrupedal robot for fast, efficient, and versatile locomotion." 15th International Conference on Climbing and Walking Robot - CLAWAR 2012, Johns Hopkins University, USA, July 23 – 26, 2012.

[9] Bledt G, Powell MJ, Katz B, Carlo J, Wensing P, Kim S, "MIT Cheetah 3: Design and Control of a Robust, Dynamic Quadruped Robot." IEEE/RSJ International Conference on Intelligent Robots and Systems (IROS), 2018: 2245 - 2252.

[10] Heglund N.C. and Taylor C.R. "Speed, stride frequency and energy-cost per stride: how do they change with body size and gait?" J. of Experimental Biology, 138, 1988, 301–318.

[11] Klaus-Dieter Budras, etc., "Anatomy of the Dog", Fifth Edition, 2007.

[12] Seok S, et al. "Design principles for energy-efficient legged locomotion and implementation on the MIT Cheetah robot." IEEE/ASME Transactions on Mechatronics 20.3 (2015): 1117-1129.

[13] Shkolnik A, et al. "Bounding on rough terrain with the LittleDog robot." The International Journal of Robotics Research 30.2 (2011): 192-215.

[14] de Viragh Y, Bjelonic M, Bellicoso CD, Jenelten F, Hutter M, "Trajectory Optimization for Wheeled-Legged Quadrupedal Robots using Linearized ZMP Constraints." IEEE Robotics and Automation Letters, 4(2), 1633-1640 (2019).

[15] Bertram, J. E., Gutmann, A., "Motions of the running horse and cheetah revisited: fundamental mechanics of the transverse and rotary gallop." Journal of The Royal Society. 6, 549-559 (2008).

[16] Maes, L. D., Herbin, M., Hackert R., Bels, V. L., Abourachid, A., "Steady locomotion in dogs: temporal and associated spatial coordination patterns and the effect of speed." The Journal of Ex-perimental Biology. 211, 138-149 (2008).

[17] Biancardi, C. M., Minetti, A. E., "Biomechanical determinants of transverse and rotary gallop in cursorial mammals." The Journal of Experimental Biology. 215, 4144-4156 (2012).

[18] Hoyt D. F., Taylor C. R., "Gait and the energetics of locomotion in horses," Nature, vol. 292, pp. 239 - 240, 1981.

[19] Turner C. H., "Three rules for bone adaptation to mechanical stimuli," Bone 23(5): 399-407 (1998).

[20] Mills D, Taylor R, Levine D, Gross D (2003). Canine IIIVET: Therapeutic Exercise Prescrip-tion/Aquatic Therapy Handbook; Charles D. Newton, "Nomal Joint Range of Motion in the Dog and Cat," University of Tennessee, Knoxvile. pp. 62-65.

[21] McDowell L, "The dog in action," Orange Judd Publishing Company, 1950.

[22] Kajita, Shuuji, et al. "The 3D Linear Inverted Pendulum Mode: A simple modeling for a biped walking pattern generation." Intelligent Robots and Systems, 2001. Proceedings. 2001 IEEE/RSJ International Conference on. Vol. 1. IEEE, 2001.

[23] Buchli, Jonas, et al. "Compliant quadruped locomotion over rough terrain." Intelligent Robots and Systems, 2009. IROS 2009. IEEE/RSJ International Conference on. IEEE, 2009.

[24] Kalakrishnan, Mrinal, et al. "Learning locomotion over rough terrain using terrain templates." Intelligent Robots and Systems, 2009. IROS 2009. IEEE/RSJ International Conference on. IEEE, 2009.

[25] Wang Z, Sun C, Deng G, and Zhang A, "Locomotion planning for quadruped robot over rough terrain." Proceedings - 2017 Chinese Automation Congress (CAC), Pages: 3170-3173, 20-22 Oct. 2017, Jinan, China.

[26] Jin B, Sun C, Zhang A, "Single leg compliance control for quadruped robots," Proceedings - 2017 Chinese Automation Congress (CAC 2017), Pages: 7624-7628, 20-22 Oct. 2017, Jinan, China.

[27] Hoyt D, Taylor R, "Gait and the energetics of locomotion in horses," Nature, 292, 1981, 239-240.

[28] Farley C, Taylor C, "A mechanical trigger for the trot-gallop transition in horses," Science, 253(5017), 1991, 306-308.

[29] Nunamaker D.M., Blauner P.D., "Normal and abnormal gait," In Newton, C.D. and Nunamaker, D.M. Eds., Textbook of Small Animal Orthopaedics, IVIS Publisher, 1985.

[30] Jin B, Sun C, Zhang A, et al. "Joint Torque Estimation toward Dynamic and Compliant Control for Gear-Driven Torque Sensorless Quadruped Robot." in IEEE/RSJ International Conference on Intelligent Robots and Systems(IROS) 2019, Nov 2019.

[31] Xiong X, Wörgötter F, Manoonpong P, "Virtual agonist-antagonist mechanisms produce biological muscle-like functions: An application for robot joint control," Industrial Robot: An International Journal, vol. 41, no. 4, pp. 340 – 346, 2014.